Exploiting ion-mobility mass spectrometry for unraveling proteome complexity

Perchepied, Stan; Zhou, Zhuoheng; Mitulović, Goran; Eeltink, Sebastiaan

Published in:
Journal of Separation Science

DOI:
10.1002/jssc.202300512

Publication date:
2023

License:
Unspecified

Document Version:
Accepted author manuscript

Exploiting ion-mobility mass spectrometry for unravelling proteome complexity

Stan Perchepied[1], Zhuoheng Zhou[1], Goran Mitulović[2], and Sebastiaan Eeltink[1,*]

[1]Vrije Universiteit Brussel (VUB), Department of Chemical Engineering, Brussels, Belgium

[2]Bruker Daltonics, Vienna, Austria

(*) Corresponding author

Pleinlaan 2, B-1050, Brussels, Belgium

Tel.: +32 (0)2 629 3324, Fax: +32 (0)2 629 3248, E-mail: seeltink@vub.be

Abstract

Ion mobility spectrometry-mass spectrometry (IMS-MS) is experiencing rapid growth in proteomic studies, driven by its enhancements in dynamic range and throughput, increasing the quantitation precision, and the depth of proteome coverage. The core principle of ion mobility spectrometry is to separate ions in an inert gas under the influence of an electric field based on differences in drift time. This minireview provides an introduction to IMS operation modes and a description of advantages and limitations is presented. Moreover, the principles of trapped ion mobility spectrometry – mass spectrometry (TIMS-MS), including parallel accumulation – serial fragmentation are discussed. Finally, emerging applications linked to TIMS focusing on sample throughput (in clinical proteomics) and sensitivity (single-cell proteomics) are reviewed, and the possibilities of intact protein analysis are discussed.

Keywords: timsTOF; Parallel accumulation-serial fragmentation, Clinical proteomics, Single-cell analysis; Data-independent acquisition

1. Introduction

The origin of protein profiling studies can be traced back to the early 1970s with the establishment of two-dimensional gel electrophoresis [1]. In 1996, the term "*proteome*" was introduced by Wilkins *et al.*, a combination of 'protein' and 'genome' [2]. Proteomics is the research discipline that aims to quantitatively characterize the comprehensive set of all proteins expressed by cells, tissue, or organism. The complexity of contemporary proteome samples is vast, with millions of different proteoforms estimated to arise from the approximately 20,000 protein-coding genes in the human genome [3]. Moreover, proteoforms' composition, concentration, and location can vary over time. In 2020, Adhikari *et al.* reported on "*A high-stringency blueprint of the human proteome*" which involves the results of ten years of proteomics research targeting to obtain a detailed molecular understanding of the dynamic nature of the proteome, its modifications, and relationships to human biology and disease, which led to the coverage 90.4% of the human proteome [4]. To maximize impact in translation, the grand challenge of the Human Proteome Project has been redefined in 2022 as the exploration of the human proteome by understanding proteins in their network environment and will enable the elucidation of its biological significance, and ultimately its function [5]. This target places stringent demands on the analytical instrumentation and workflows employed for their analysis, as this not only involves quantitative proteomics research but also targets the characterization of protein structures and assemblies, including protein-protein interaction networks.

Liquid chromatography–mass spectrometry (LC-MS) plays a critical role in proteomics research as it enables the separation, comprehensive identification, and high-sensitivity quantification of proteins. Different MS-based approaches can be distinguished for protein characterization. Top-down proteomics involves the analysis of intact proteins that are first separated using reversed-phase liquid chromatography (RPLC), after which the separated

proteins are transferred online into the mass spectrometer via electrospray ionization (ESI) [6]. MS analysis involves either the determination of the mass of the intact proteins based on high-resolution MS or the elucidation of the protein sequence can be based on gas-phase fragmentation. Top-down proteomics has only found limited applications for protein sequencing, mainly because of its low throughput as fragmentation conditions are not straightforward and the difficulties encountered when assessing multiplexed MS spectra. Bottom-up LC-MS proteomics, also named shot-gun proteomics, is considered the current gold standard for protein sequencing [7]. The typical bottom-up workflow involves the subsequent reduction, alkylation, and digestion of proteins, before an ion-pairing RPLC separation of resulting peptides using formic acid as additive yielding adequate ionization efficiency. Consequently, peptides are introduced in the MS via ESI. Subsequent tandem mass spectrometry (MS/MS) analysis typically involves collision-induced dissociation of peptides allowing the determination of the amino-acid (AA) sequence. The identity of proteins can be retrieved by unambiguously identifying one or two tryptic peptides with distinct sequence(s). Middle-down proteomics was developed in the early 2000s. It involved the characterization of cleaved or truncated protein fragments that are slightly 'longer' (20-100 AA residues) proteolytic peptides than the ones usually obtained in bottom-up studies (7-20 AA residues) [8]. This workflow is anticipated to allow the detection of more unique peptides (particularly of greater lengths) that enhance the sequence coverage and, in turn, would lead to the identification of a higher number of post-translational modifications compared to the classical bottom-up approach.

Ion mobility (IM), described more than 100 years ago by Rutherford [9] has emerged as an integral part of proteomics research. IM enhances selectivity as ions are separated in the gas phase based on mass, charge, and shape difference [10]. Moreover, MS detection sensitivity can potentially be increased as IM-MS adds an extra separation step in comparison to

standalone MS, where gaseous ions are concentrated and isolated based on their ion mobility prior to MS sampling. Major hardware developments included the interfacing of the IM drift tunnel orthogonally to a time-of-flight mass spectrometer (IM-TOF) McAfee and Edelson [11] and the introduction of the first commercial IM-MS by the Franklin GNO Corporation [12]. Various modes of IM have been developed and commercialized, each with its specific design [13]. Four notable designs, namely drift tube ion mobility spectrometry (DTIMS), high-field asymmetric-waveform ion mobility spectrometry (FAIMS), traveling-wave ion mobility spectrometry (TWIMS), and the recently emerging trapped ion mobility spectrometry (TIMS), have demonstrated successful integration with high-resolution mass spectrometers. This review introduces IM fundamentals and describes the main modes of IM operation. Moreover, the hardware of an emerging proteomics platform, *i.e.*, the timsTOF MS, is discussed, and key proteomics applications are reviewed.

2. Fundamentals in ion-mobility spectrometry

2.1. Principles

IMS is a separation technology based on the differential migration of ions in inert buffer gas under the influence of an electric field. Considering a cluster of ions drifting along an electric field in a gas-filled tunnel, the driving force of the ion movement is the net outcome of the conservative electric force and the nonconservative friction force due to the resistance on the path caused by the collisions with the buffer gas (analogy to "*parachuting model*") as exemplified by Gabelica *et al.* [14]. When a steady state is reached, the ions will migrate with a constant velocity $\overrightarrow{v_d}$, which is a function of the electric field applied $\vec{E}$, and their ion mobility *K*.

$$\overrightarrow{v_d} = K \cdot \vec{E} \quad (1)$$

Ion drifting is directly affected by the electric field driven acceleration and the collision-induced friction. Consequently, ion mobility on a molecular level can be described in association with the ion electric properties and its collision behavior with the buffer gas. This fundamental relationship was first established by Langevin [15], and later refined by Mason and Schamp as [16]:

$$K = \frac{3q}{16N} \cdot \left(\frac{2\pi}{k_B T}\right)^{\frac{1}{2}} \cdot \left(\frac{1}{m} + \frac{1}{M}\right)^{\frac{1}{2}} \cdot \frac{1}{\Omega} \quad (2)$$

where q is the ionic charge, N is the buffer gas number density at the given temperature (T), k_B is the Boltzmann's constant, m and M are the masses of the buffer gas and the ion respectively, and Ω is the collision cross section (CCS). Ω represents the momentum transfer collisional integral, which describes the averaged ion-gas pair momentum transfer over all thermal velocities. It depends not only on the summed radii of the ion-buffer gas pair, but also on the ions pair's short-range interaction potential and polarizability [17]. Since Ω is expected to have a dimension of an area (square angstrom), it is sometimes described as the gas-phase ion size (which is structure dependent) [18]. This analytical expression of ion mobility depends on the experimental conditions (N, P, T). As it is challenging to compare ion mobility for different instruments and measuring conditions, reduced ion mobility (K_0) has been introduced, which is normalized to standard gas conditions:

$$K_0 = K \frac{N}{N_0} = K \frac{p}{p_0} \frac{T_0}{T} \quad (3)$$

where p_0 = 1 atm, T_0 = 273.15 K. Because K is independent of $\vec{E}$ only when a low electric field is applied the energy acquired from the electric field is negligible to the thermal energy of the buffer gas, and the ion motion is dominated by diffusion. In high-field IMS, the energy gained from the electric field is much greater than the thermal energy, and the ion mobility should be

expressed as the function of the electric field and gas density ($\vec{E}/N$ *i.e.*, reduced electric field in Townsend's units (Td), 1 Td = 1×10^{-17} V·cm^2) as a power series as:

$$K = K_0 \cdot (1 + \sum_{n=1}^{\infty} \alpha_{2n} \cdot \left(\frac{\vec{E}}{N}\right)^{2n}) \quad (4)$$

where α_{2n} are the specific constants for different ions. Expression 4 is also named as α function. In high-field IMS (*e.g.,* FAIMS), the separation of ions relies on this unique property, since it is the K/K_0 ratio (as a function of α_{2n}) instead of the K_0 or CCS that has been measured [19]. The onset threshold where low-field IMS turns into high-field IMS is discussed in [20].

2.2. IMS operation modes

A comprehensive comparison between the different IMS operation modes has been well reviewed [18,21–23]. As such, this section intends a short introduction to all of them. A summary of the principle of operation, the main advantages and limitations are described in the following paragraphs and summarized in Table 1.

Drift tube ion mobility spectrometry (DTIMS) is considered the most straightforward IM configuration, see Fig. 1A for the schematic representation of the separation principle. Ions are accelerated through the drift tunnel thanks to a low-strength electric field. The ion-mobility hardware consists of ring electrodes along the linear drift tunnel, which allows for generating a uniform low static electric field of approximately 1 to 15 Td [14]. Ions are accelerated in the opposite direction of the drift gas, flowing from the outlet to the inlet of the drift tunnel, providing frictional forces. As a time-dispersive IM, all ions will sequentially follow the same separation path and hit the detector at the same place according to their separation velocity, and the drift time (t_d) of the analytes is monitored. CCSs can be retrieved via the Mason-Schamp rule (Eq. 2) without the need for calibration. High separation resolutions of approx. 100-200 t_d / Δt_d can be achieved, but the performance depends on tunnel length, pressure, and the type of

gas applied [24]. A significant drawback of this configuration is that ions are injected into the drift tunnel in periodic pulses. Hence, a 100% duty cycle cannot be attained. For most of the experiments, the ions are trapped for a duration of only 4 ms before being separated in the drift region for 60 ms, which results in a duty cycle of 6.7% [18]. All other ions deviate from the detector during the separation step, and potential information is lost. The duty cycle can be increased up to 50% thanks to deconvolution post-data processing. Indeed, applying deconvolution techniques (*e.g.*, Fourier and Hadamard transformations) results in a spectrum containing a higher signal and mobility values which allow to run faster separation steps [25]. The DTIMS separation principle is based on the ion mobility that relates to both the shape of molecules and its mass [21].

Traveling wave ion mobility spectrometry (TWIMS) utilized a similar separation principle as DTIMS, but the configuration incorporates ring electrodes where a waveform-like electric field is created, [26]. Like DTIMS, the drift tunnel is filled with drift gas flowing from the outlet to the inlet of the drift tunnel, and this mode is described as time-dispersive IM. The drift time must be calibrated to obtain CCSs values for a given condition, *e.g.*, wave height and frequency, gas pressure, and gas type [27]. An advantage of TWIMS compared to DTIMS is the size of the instrument for comparable resolving power, as TWIMS requires shorter drift tunnels. Even though high resolving power (R) has been obtained with long drift tunnels (R = 400 [28]), most of the instrument configurations are limited to R = 50 [22], which is generally lower than with the DTIMS. Smith and coworkers developed traveling wave-based structures for lossless ion manipulations (TW-SLIM) module, which allows for high IMS resolution [29]. Another major limitation of TWIMS is the electric field heating that may induce dissociation or isomerization of proteins [30]. These structures only exist due to the experimental conditions applied and do not represent the ones observed in a biological sample. Thus, the instrument is proving to be limited when studying native-like biomolecule structures.

Table 1. Description of IM modes, features, and advantageous/disadvantages, adapted from [19].

	DTIMS	TWIMS	DMA	FAIMS	TIMS
IM mode	Time dispersive	Time dispersive	Spatial dispersive	Spatial dispersive	Ion confinement and selective release
Instrument	- 6560 Ion mobility Q-TOF - IMS-TOF	- Synapt G2-Si - Vion IMS Q-Tof	- mobility front-end	- FAIMS interface - SelexION - Ultra FAIMS	- timsTOF
Features	- Static electric field - No gas flow	- Oscillating electric field - No gas flow	- Static electric field - Perpendicular gas flow	- Oscillating electric field - Parallel gas flow	- Static electric field - Parallel gas flow
Advantages	- The electric field across the drift tunnel is uniform which makes the K directly related to $t_{d.}$ CCCs can be determined without calibration - Used for calibrants with well-characterized CCS of other IM modes - Sequential collection / separation step means that all ions	- Sequential collection / separation step means that all ions which are separated are detected - Longer drift lengths than in DTIMS due to the wave-like voltage) yield increased resolution	- Can carry out measurements of a large ion mobility range and is typically used for the analysis of macromolecules (approx. tens to hundreds of nm^2) - Scannable operation mode makes it an alternative to use as an ion filter	- The shape of the ions is altered between the high / low electric field The IM separation is not only based on the shape of the ions which strongly correlates to its mass - Scannable operation mode makes it an alternative to use as an ion filter - Continuous collection of data	- Successive elution of ions by lowering the electric barrier yields high resolution (up to R ~ 200) - Slower scans are more selective and are more capable of separating analytes with similar mobilities than faster scans, yet faster scanning may be necessary for

		which are separated are detected			means no loss of information	high throughput analyses. - Dual TIMS operation: collection during separation and yields a duty cycle up to 100%
Limitations	- Limited resolving power (R ~ 80) - Sequential collection / IM separation: duty cycle is limited at 50% if the time of collection and separation are equal	- Superposition of wave-like voltage pulses on which ions are moved means that *K* needs to be first related to t_d according to experimental conditions. CCSs are only obtained upon calibration - Sequential collection / separation step means that the duty cycle is limited at 50% if the time of collection and separation are equal	- Scannable operation mode means that only the ions with the targeted mobility will be directed towards the detector and ions with diverse mobilities cannot be detected at the same time	- The shape of the ions is altered between the high / low electric field means that no CCS can be determined (directly nor indirectly) - Scannable operation mode means that only the ions with the targeted mobility will be directed towards the detector and ions with diverse mobilities cannot be detected at the same time	- Risk of space charge effects with complex samples result in lower sensitivity - Little studies about the coupling with very high-resolution MS (FTICR)	

Differential mobility analyzer (DMA) is a space-dispersive IM mode, see Fig. 1B for its separation principle. All ions will follow different separation paths and hit the detector simultaneously but at different places according to their separation path. The instrument setup combines a constant electric field and an orthogonal gas flow [18], and ions are moved between planar electrodes. Depending on $\overrightarrow{v_d}$, only those ions with the appropriate mobility will reach the exit cell. The other ions will collide with the electrode, preventing their detection. By scanning the electric field, an ion spectrum reflecting the distinct ion mobilities is recorded. DMA is considered a selective filter.

High field asymmetric waveform ion mobility spectrometry (FAIMS) is a space-dispersive IM mode, where ions oscillate between two electrodes with applied low and high electric fields and travel in a gas flow parallel to the electric field, see Fig. 1C. Similarly, as DMA, FAIMS acts as an ion filter. Depending on the strength of the electric field, only selected ions that do not collide with the electrodes will be detected, in close analogy to quadrupole mass filters. The difference with a quadrupole mass filter is the presence of the gas which will add a separation dimension by the transmission of the ions based on mass, shape, clustering between ions with the neutral gas molecules, and the dipole moment [31]. The main advantage of FAIMS is that due to a separation of ions between high and low electric fields, the instrument is more orthogonal than DTIMS, or TWMS, to MS as they rely directly on a difference of mobility in low electric field [21]. At low field strengths, an ion's mobility is independent of the applied electric field. However, in high electric fields the mobility of an ion changes with electric field strength. It causes it to exceed the low-field limit and therefore prevents the correlation of drift time with the shape, as the mobility of an analyte is not directly related to its structure [22]. Furthermore, it has been observed that the Coulomb repulsion of ions due to inhomogeneous filling between the electrode can cause ions to focus/defocus from the middle of the ion path, which results in lower MS sensitivity [30].

Trapped ion mobility spectrometry (TIMS) is the most recent operation mode developed for ion mobility, and its separation principle is displayed in Fig. 1D [32]. In TIMS, a specific IM mode consisting of ion confinement and selective release is applied. The IM device is divided into two regions: an ion-trapping tunnel for parallel ion accumulation and an IMS tunnel separating ions packets [33]. The drift gas and the electric field within the instrument are oriented in opposite directions. The electric field gradient is created along the trapping tunnel to immobilize the ions at different positions according to their *K* (*i.e.*, where the electrical force compensates for frictional forces). Ions are sequentially eluted towards the drift tunnel by lowering the electric field strength. Since IM is performed in the range of hundred milliseconds, it is optimally suited for hyphenation to fast and mass-accurate qTOF instruments (cycle time of approximately 100 μs). The mobility-separated ions can be displayed on a heat map of the ion mobility expressed as $1/K_0$ drift time *vs. m/z* [34].

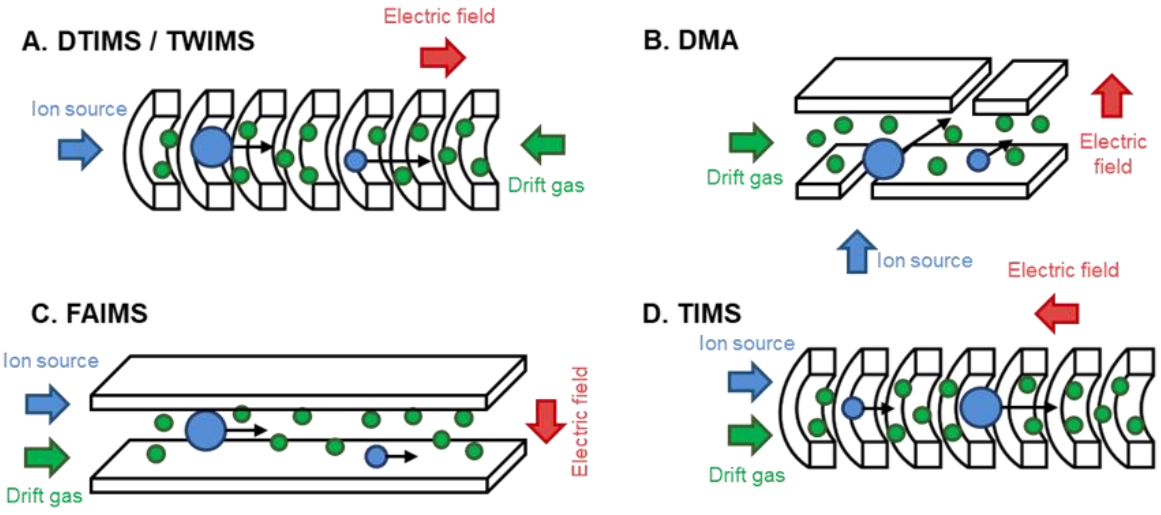

Figure 1. Schematic representation of the basic operational principle of ion-mobility modes covered in this review: **(A)** Drift tube ion mobility spectrometry (DTIMS) and traveling wave ion mobility spectrometry (TWIMS). **(B)** Differential mobility analyzer (DMA). **(C)** High field asymmetric waveform ion mobility spectrometry (FAIMS). **(D)** Trapped ion mobility spectrometry (TIMS). Arrows indicate the orientation of the ion source (blue) as well as the

direction of the forces from the drift gas (green) and the electric field (red) are highlighted for each mode.

2.3. Ion-mobility-based resolving power

Similar to other analytical separation technologies, the differential location of ion packets (peak) in IMS provides the basis of qualitative information on analytes. Depending on operation modes, ion packets are temporally (DTIMS/TWIMS *vs.* high-performance liquid chromatography/capillary zone electrophoresis) or spatially (FAIMS/DMA *vs.* isoelectric focusing/imaged capillary zone electrophoresis) separated, or in a combined manner (TIMS *vs.* isoelectric focusing in elution mode). Although the aforementioned IM operation modes separate ion packets differently, the separation performance can still be described and compared by analyzing mobilograms (the counterpart of chromatograms in chromatography, which display the mobility of ions) and peak properties.

The resolution, *R*, in different IMS configurations, has already been extensively reviewed [35–38]. *R* is dimensionless ($t/\Delta t$) for DTIMS and TWIMS, ($Hz/\Delta Hz$) in overtone IMS and cyclic IMS, and ($V/\Delta V$) in FAIMS and K_0 ($cm^2 \cdot V^{-1} \cdot s^{-1} / \Delta\ cm^2 \cdot V^{-1} \cdot s^{-1}$) in TIMS. It allows for, (a) comparing IMS performance across different instrument configurations, (b) predicting the required resolving power with given CCS differences to achieve separation with fixed resolution, and (c) predicting the separation possibility for a specific group of ions with given *R*. The resolution of state-of-the-art IMS instruments generally range between 50 to 300 [39], which permits baseline separation with IM differences as low as 0.4%. As IM-based resolving power is orthogonal to the hydrophobicity-based separation by reversed-phase LC and semi-orthogonal to the *m/z*-based differentiation by MS (as Ω often increases with the mass),

the hyphenation of LC-IMS-MS provides unique possibilities to assist deeper mining of biological information for proteomic research:

- *Noise removal* by excluding the small molecule contaminants to increase the sensitivity and dynamic range of MS [40,41].
- *Alleviating the classic "co-fragmentation" problem* in MS/MS experiments by differentiating isobaric precursors on mobilograms and increasing identification confidence [42–45].
- *Structural conformation* of a single protein or a protein network through evaluation of the CCS [46–48], allows to obtain information about intramolecular forces [49,50].
- The s*tructural heterogeneity of proteins and complexes* can be determined using the information on peak dispersion. For instance, a sharp peak will indicate the presence of a single or limited conformation, while a broader peak will be informative on the presence of additional structural conformations [51].
- *Stability and intermediate folding states* can be determined by processing analyses over a wide range of collision energies for different CCS values. The result is a fingerprint upon which interactive proteins and proteins isoforms may be visualized [52].
- *Prediction of peptide CCS* can improve confidence of MS/MS-based identification and contributes to the better understanding of the IMS mechanisms [53].

3. Trapped ion-mobility spectrometry time-of-flight mass spectrometry

3.1. Trapped ion-mobility spectrometry

In 2011, Fernandez Lima *et al.* successfully integrated the TIMS with a qToF and demonstrated high resolving power for isobaric small molecules with $R > 50$ [54,55]. The choice of the mass analyzer was justified by the fact that fast TIMS separation were acquired

in 25 ms (full width at half maximum was approx. a few ms) and that under these conditions, qToF can acquire data at a rate of 10 spectra ms^{-1} [56]. As the IM separation time frame was nested well in between LC separation (considering a standard proteomic LC separation (with a 90 min gradient that results in peak widths of approx. 10 s) and MS analyzer acquisition, the incorporation of TIMS module in conventional LC-high resolution MS instrumentation becomes a natural adoption. This approach was initially implemented by Meier *et al.* [34] and has been successfully commercialized.

A schematic of the timsTOF Pro ion optics, which was first described by Meier *et al.* in 2018 [42], is depicted in Fig. 2. Ion packets enter the MS instrument via an orthogonal ESI configuration. This solution helps to improve the robustness of the analyses by diverting neutral analytes and contaminants from the inlet. The charged ions focus at the entrance funnel, increasing the number of ions at the same location and improving the sensitivity, after which they are separated in the TIMS tunnel according to their differences in mobilities. The separation tunnel in TIMS instruments consists of 4 concave electrodes where the application of an RF voltage confines ions. Recently, the development of convex electrodes that, according to the authors, extend the mobility range up to 1 MDa can be used to study the macromolecular assembly of proteins [57]. Afterwards, ions are guided to the fast-switching quadrupole mass filter, which is synchronized with the TIMS by passing through an exit funnel. The ions can then be fragmented in the collision cell and detected using an orthogonal-TOF analyzer.

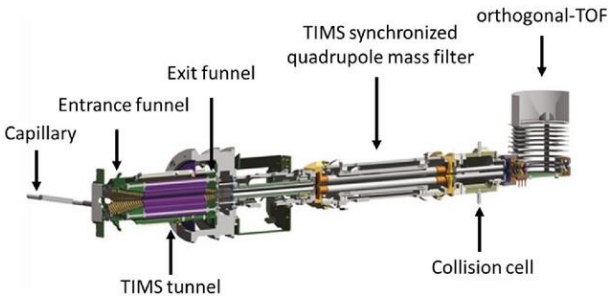

Figure 2. Configuration of the timsTOF ion path including the TIMS tunnel, where ions are separated according to their mobility, a quadrupole for selecting precursor ions, a collision cell, and a high-resolution TOF analyzer. Adapted from [92], with permission.

The core concept of the TIMS is closely related to that of drift-tube IMS and relies on the interaction of ions in a gas phase with a gas flow from the inlet to the outlet and an electric field in the opposite direction [57,58]. Depending on the interaction between the two forces, the ions will be trapped in the separation tunnel at different positions (Fig. 3A). Ions with the highest mobility will be trapped close to the inlet of the separation tunnel because they require a higher electric field to equilibrate with the frictional force. Conversely, ions with the lowest mobility will be trapped further along the separation tunnel. By sequentially lowering the energy barrier, the ions will elute toward the TOF detector, starting with the one with the lowest mobility. An advantage of the TIMS mode is that it increases the effective drift length with a fast counter flow that pushes the ions back instead of increasing the length of the drift tunnel [59].

In the analyzer section of the TIMS tunnel, see Fig. 3A, the electric field strength is spatially and temporally varied. Spatially, it increases along the length up to a maximal value E_0 where it reaches a plateau. The electric field profile is decreased in time at a rate β. Bleiholder described the electric field for every position (z) and time (t) as [60]:

$$E(z,t) = \begin{cases} \frac{z}{z_p}\,(E_0 - \beta \cdot t)\;;\; \forall z < z_p \\ E_0 - \beta \cdot t\;;\; \forall z \geq z_p \end{cases} \quad (9)$$

where z_p is the position at which the electric field reaches its maximal value E_0. Whereas the electric field in the common TIMS instrumentation decreases linearly in time, Benigni *et al.* reported the programming of a nonlinear ramp, allowing to increase the duty cycle (from 0.5% up to 4%) [61], leading to a six-fold decrease in total analysis time.

The buffer gas velocity is controlled by applying a pressure difference between the inlet and the outlet of the separation tunnel (*e.g.*, a few millibars). It remains constant throughout the analysis, resulting in a laminar parabolic flow profile due to friction near the wall [62]. Due to the parabolic profile, the ions are spread along the cross-section of the separation tunnel. Applying an RF electric field with a higher amplitude counteracts the axial spread by confining the ions to the central region of the TIMS separation tunnel. Silveira *et al.* reported CFD simulations showing that this region's gas velocity is near homogeneous [63]. A limitation of a standard TIMS instrument configuration is that the analysis is segmented, *i.e.*, trap and release. During the released operation, an electric barrier prevents the ions from entering the drift tunnel. Considering the same trapping and released time, no more than half of the ions can be analyzed. To overcome this limitation, Silveira *et al.* designed a dual TIMS configuration [64]. In this configuration, two TIMS separation tunnels are aligned in series and separated by an electric barrier (Fig. 3B). The ions are trapped in the first TIMS. An electric pulse is applied to lower the barrier between the TIMS, and all trapped ions are transferred at once in the second TIMS. Successive release of the ions is then carried out while trapping a new set of ions in the first TIMS. The advantage of this configuration is mainly an increase in the signal to noise ratio [64,65]. The latter technology has been commercialized as parallel accumulation – serial fragmentation (PASEF) and is now integrated into proteomics LC-MS workflows.

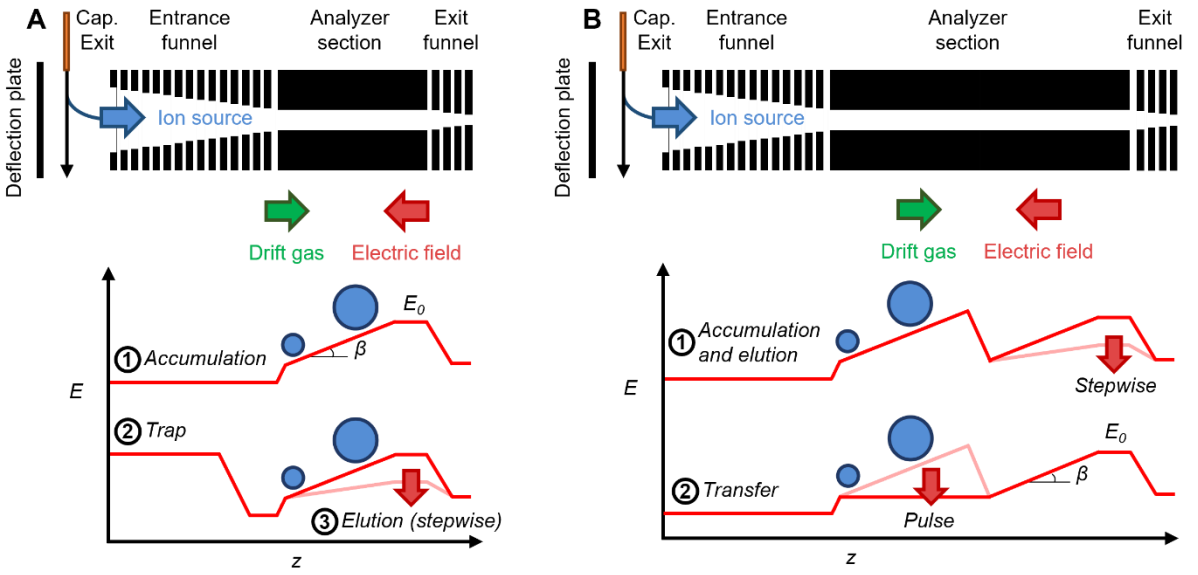

Figure 3. Schematic representation of the ion-optic elements of **(A)** the single TIMS configuration allowing sequential analyses and **(B)** the dual TIMS configuration allowing parallel accumulation / analyses. (*Top*) The orientation of the ion source (blue) as well as the direction of the forces from the drift gas (green) and the electric field (red) are highlighted. (*Bottom*) Corresponding electric-field strength to scale in the different positions of the TIMS ion optic elements as a function of the separation step (accumulation, trapping, and elution) and the axial position (*z*). Adapted from [84], with permission.

3.2. Parallel accumulation – serial fragmentation

For most of the MS/MS experiments that involve quadrupole precursor selection, the MS/MS scan speed and sensitivity can hardly be balanced since the ion accumulation takes a considerable amount of time and low abundant precursors often requires repeated sampling to achieve the desired MS/MS spectrum quality for data processing. The TIMS separation before quadruple selection partially alleviates this problem by lining up the precursors based on their ion mobility. Thus, ions with the same ion mobility were "preconcentrated" into a single ion packet (IM peak) before quadrupole selection. Yet, within a typical TIMS separation window

of 25 to 200 ms, not all IM peaks with peak widths of several ms can be selected and fragmented if the quadrupole switching between different mass selection RF and DC voltages is too slow. To further improve the precursor coverage, a novel acquisition scheme, "parallel accumulation – serial fragmentation (PASEF)" was developed [34,42], which fully synchronizes the ion-mobility separation and quadrupole precursor selection, resulting in significant improvement on acquisition speed without compromising sensitivity.

The critical technological advancement of PASEF for high-throughput MS/MS sampling is the rapid switching of quadrupole voltages to ideally accommodate all IM precursors eluted during a single TIMS scan, which is implemented by controlling the RF and direct DC via a real-time field-programmable gate array instead of the slower serial interface. The switching time of each *m/z* position on the quadrupole is thus reduced to sub-milliseconds thanks to faster communication speed than the traditional serial interface, which matches the peak widths of most IM peaks. In addition, to advance spectrum quality for low-abundant precursors and to maximize precursor coverage, a heuristic searching algorithm was developed concomitantly with dynamic exclusion, by deliberately "re-sequencing" these low abundant species in consecutive PASEF scans and accumulating all the spectrum until the intensities reach the target threshold. With this new MS/MS scheduling approach, after parallel accumulation and sequential release of ion mobility packets from the dual TIMS chamber, several PASEF scans are scheduled in sync with the IM elution, and multiple precursors are selected and fragmented within single PASEF scans based on *m/z* and intensity. The overall MS/MS scanning speed can be 10-fold higher than the conventional top-*N* approach (*N* refers to the number of precursors). Up to 100 Hz scanning speed is achievable without compromising sensitivity, which significantly enhances the depth of the proteome coverage in a shot-gun workflow, which is of great importance especially when targeting applications that require high sample throughput or when analyzing small sample amounts.

3.3. dia-PASEF and X-PASEF

The first few demonstrations of the PASEF workflow were implemented in a data-dependent acquisition (DDA) manner [42], which requires the predetermination of ion mobility, mass-to-charge ratio, and intensity from the previous TIMS scan. Only a finite number of precursors can be selected and fragmented at any LC elution time. Still, the advantageous separation capability of TIMS and the fast precursor selection speed on the quadrupole, allows the PASEF approach to be extended to a data-independent acquisition (DIA) scheme, or other advanced acquisition schemes with the minimum if no hardware modifications [43]. To increase the dynamic range of precursors sampling, DIA, as an alternative MS/MS experiment approach, was established in the early 2000s [66]. This approach intrinsically does not require any pre-known information on the precursor ions from survey scans, and theoretically, all the precursors are sampled without any systematic bias.

In DDA mode, a narrow *m/z* window is set on the quadruple per each fragmentation event scheduled, allowing precursors to be transferred to the collision cell, which produces tandem spectra exclusively assigned to the selected precursors. In contrast, quadrupole voltages in DIA are alternated stepwise with relatively broad, user-defined *m/z* windows, where all precursors falling in the range will be fragmented, overcoming the biased and incomplete sampling. However, the complexity of the MS/MS spectra poses a significant challenge to the data analysis algorithms [67]. Even though the DIA acquisition can comprehensively sample all the precursors, the sampling efficiency of individual precursors is expected to be low. Since each *m/z* isolation window is often maintained narrow (generally from 10 to 25 Th) to avoid extremely complex MS/MS spectra, yet a rather wide m/z range (from 400 to 1200 Th) must be traversed to cover all charged peptides-like species. Thus, each DIA cycle consists of 32 to 80 stepping windows. Suppose the precursor selecting quadrupole is switched with rather slow

speed, then the cycle time is inevitably increased, where the sampling efficiency of each precursor is reduced during the LC elution timespan.

Considering the separation capability of TIMS and the controllable nature of quadrupole selection of PASEF, dia-PASEF is devised with modifications on the instrument control electronics allowing seamless ramping of the voltages for all isolation windows and adjusting collisional energies according to IM. The extra separation dimension of TIMS provides "cleaner" ion packets for every fragmentation event, which allows for using a relatively large isolation width with fewer stepping windows required. The rapid and IM-synchronized quadrupole switching also enables more isolation windows to be utilized on the *m/z* – IM plane within the cycle time to further increase the sampling efficiency, and a duty cycle of 100% is even possible to be achieved.

Thanks to the fast and controllable nature of quadrupole positioning and the extra separation dimension of IM, a broad range of more sophisticated acquisition schemes can be designed on a timsTOF Pro instrument in a DIA manner. To further enhance the precursor sampling completeness, Slice-PASEF [68] was developed. The isolation window can be stepped in an overlapping manner. This leads to increased selectivity for alternatively overlapping, and larger isolation windows. Synchro-PASEF [69] was developed to re-route of digital-to-analog converters of the quadrupole RF amplitude, the bias DC, and the resolution DC on the field programmable gate array, enabling a fast and continuous quadrupole movement. Instead of statically ramping the isolation window stepwise, this quadrupole movement allows the fixed isolation window to traverse diagonally over the *m/z* – IM plane in a "scanning" mode with very narrow IM spacing and small *m/z* increments. More recently, Distler *et al.*, demonstrated the possibility of combining Slice-PASEF and Synchro-PASEF (Maximizing Information content in dia-PASEF, Midia-PASEF) to further increasing the sampling efficiency and reducing the cycle time [70].

4. Selected key applications

4.1. Bottom-up proteomics

Empowering simultaneous and quantitative determination of thousands of proteins in tissues and biofluids, comprehensive proteomic profiling has asserted its role across various applications, from signaling pathway in immunology to pathology in precision medicine [71,72]. One of the key technologies is LC-MS based shot-gun proteomics, where sample proteins are digested into peptides prior to analysis. The peptides are chromatographically separated and ionized followed by tandem MS sequencing. The sequence information of peptides will be collectively compared and scored against the in-silico generated spectra database, to produce candidate lists of peptides and consequently proteins. The MS intensity information is retrieved and compared between samples for quantitation in either labeled or label-free manner.

To ensure in-depth coverage of proteome within affordable analysis time, technical advancements have been focused on (1) improving LC resolving power to minimize ion-suppression induced biased sampling and co-fragmentation (co-eluted precursors with similar *m/z*), and (2) accelerating tandem MS spectra acquisition speed to cover the majority, if not all of peptide precursors from the upstream. These parallel developments have significantly boosted the protein identifications and analysis speed from about one hundred protein groups identified in 24 hours at the turn of this century [73], up to 5000 protein groups within 90 min reported by Mann's group a decade ago [74]. In 2018, the landscape of bottom-up proteomics has been further refined since the advent of IMS implementation in LC-MS instrumentation for proteomic profiling, where around 6000 protein groups have been identified in 2 h by the same group [42]. These advantages do not only improve the conventional discovery proteomic workflow with more confidence on data quality and reproducibility, but also decreases the limits of proteomics to accommodate ultrashort runtime in high throughput proteomic assay

and limited sample amount in single cell analysis, which are separately discussed in the below sections.

4.1.1. High-throughput proteomics

Beyond successful applications in fundamental research, shot-gun proteomics has also found growing interests for biomarker discovery in clinical environment and drug screening in biopharmaceutical industry. As these analytical tasks are often encountered with large sample cohorts, it is not only coverage depth, quantitative precision, but also analysis speed that is increasingly demanding. Limited by tandem spectra acquisition speed, the well-established discovery proteomic workflow is largely relying on the high-quality peptide separation, which generally involves the use of long columns and long gradient times (3 h and longer). This combined with the extensive time required for sample preparation and data processing results in diminishing returns on protein identifications, making such platform unaffordable for high-throughput proteomic profiling. The advancement of ultra-high-performance liquid chromatography (UHPLC) technology has revolutionized the field by allowing the use of shorter gradients. This breakthrough has resulted in a higher peak-capacity- per-unit time and reduced average peak width. Consequently, the cycle time of MS also needs to be reduced accordingly to achieve enough data points per eluted LC peak for accurate quantification [75].

The concept of utilizing fast high-quality chromatographic separations in combination with short MS duty cycles has been discussed during the introduction of PASEF scheme in '*Section 3.3*'. With standard TIMS ramping time of 100 ms and 10 dda-PASEF scans per duty cycle, an average 3470 protein groups were identified in one hour from 100 ng HeLa with median CV below 18% [42]. Extremely fast analysis has also been showcased, where 1231 protein groups are identifiable within a total analysis time of only 7.2 min [42]. With dia-PASEF acquisition scheme applying a reduced cycle time of 0.9 s, the same research group has

also demonstrated the quantitative identification of around 5000 protein groups in 21 min LC time with a median CV of 5.8% [43].

Szrywel *et al.* reported the analysis of blood plasma using the analytical flow of 500 µL/min and 850 µL min^{-1} in a dual column setup and DIA MS method termed Speedy-PASEF [76], enabling the analysis of 236 samples per day and 398 samples per day for the dual gradient setup. Authors described the use of two different ionization sources and selected the ion source with the heated electrospray for reasons of better desolvation and ionization. This group also systematically investigated the impact of sample input considering protein mass, and gradient duration on protein identification and reproducibility for high-throughput proteomics, see Fig. 4. The number of identified proteins and peptides with the three-minute separation gradient was reported to be 1589 proteins and 5591 precursors for 10 ng of HeLa digest. Furthermore, the CV for protein quantitation was maintained at 16% for the 10 ng injection.

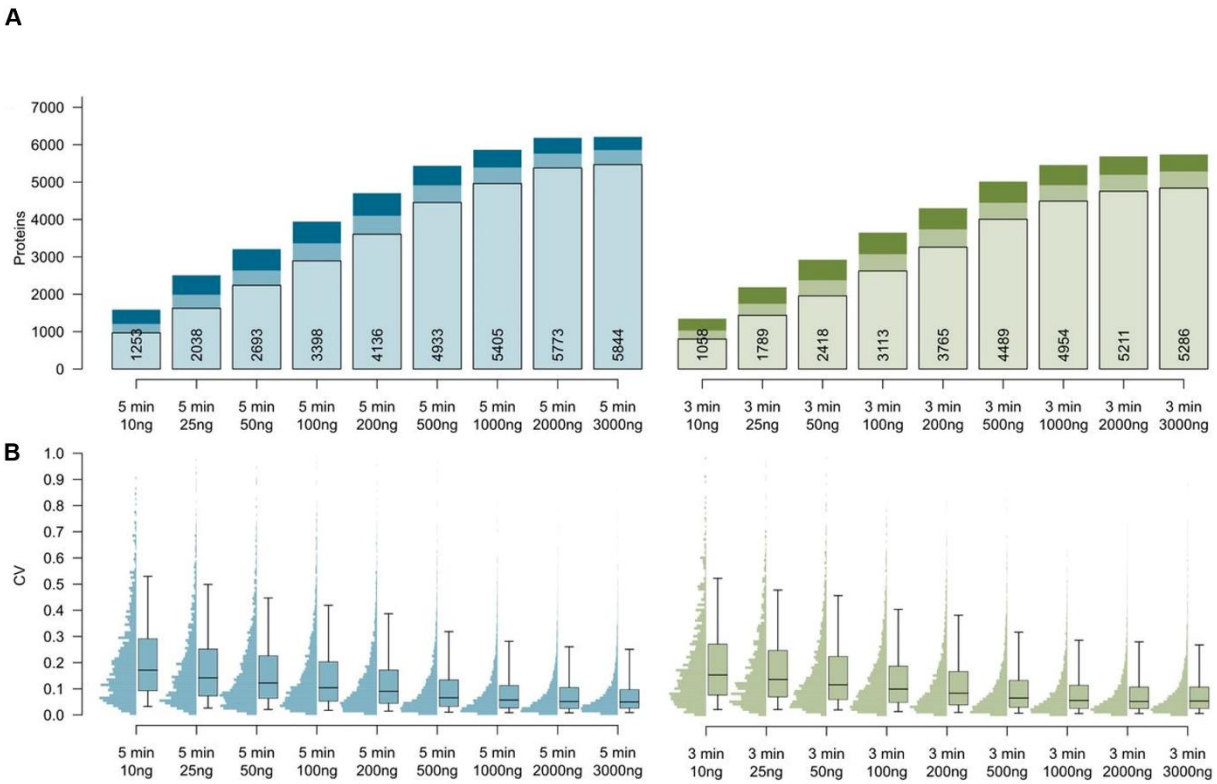

Figure 4. Performance characteristics of UHPLC-timsTOF applying analytical flow rates and short gradients. **(A)** Numbers of quantified proteins for different injection amounts of a K562 tryptic digest analyzed with a 5-minute (*left*) or 3-minute (*right*) analytical flow gradient (500 µL/min). Proteins detected in 1, 2, or all 3 injection replicates for each amount are shown with different color shades; average numbers are indicated. **(B)** The respective coefficient of variation distributions. The boxes correspond to the interquartile range, with the median indicated, and the whiskers extend to the 5-95% percentiles. Adapted from [76] with permission.

Combining capillary-flow LC and optimized dia-PASEF settings, even higher sample throughput was demonstrated by Tomioka *et al.*[77]. Authors claim that they were able to identify more than 3000 proteins from the 100 ng of tryptic HeLa peptides and more than 2000 protein groups from 10 ng of HeLa. The CVs of the retention time, peak intensity, and the number of identified peptides when injecting a higher centration of 500 ng HeLa digest for 100 times were on average 3.4%, 19.8%, and 6.0%, respectively. Optimization steps finally led to

a gradient separation method with 0.8 minutes gradient and 10 µL/min flow rate, which enables the analysis of 1000 samples per day. Quantitation CV was less than 20% across samples. These workflows demonstrate the potential of utilizing timsTOF for high-throughput proteomics in a more efficient manner, reducing both time and cost.

4.1.2. High-sensitivity / single-cell proteomics

The conventional proteomic assays based on population average of an organism, or of a tissue sample, capture only the primary biological mechanisms operating within cells, but do not distinguish the heterogeneity in functions or composition of the cell population. However, understanding of substructures of biological tissues (tumor microheterogeneity, embryogenesis), tumor microenvironments (cell signaling, regulatory networks), rare-cell populations (circulating tumor cells) can only be realized by differential characterizations of proteomes on a single-cell level. The challenge of analyzing the proteome of the single cell lays in the fact that the amount of protein estimated to be present in a single cell is about 100 to 200 pg. Over the past ten years significant efforts have been made on single-cell handling, miniaturized sample preparation and integrating labeling techniques [78], aiming to minimize sample loss prior to instrumental analysis. Sub-narrow bore columns (i.d. < 50 mm) have also been developed concomitantly to reduce LC-induced dilution and to boost ionization efficiency while operating at ultra-low flow regime (< 50 nL min^{-1}) [79].

The rise of single-cell proteomics should also be attributed to the sensitivity improvement in MS instrument designs. Besides the re-engineering in ion-optics and transmission tunnel to enhance the ion utilization, the introduction of IMS also played an indispensable role in MS sensitivity improvement, The “concentrating” effect after IMS elution enables signal/noise ratio enhancement in each MS duty-cycle and more importantly, the IMS differentiation of singly-charged contaminants and multiply-charged peptide-like features

makes tandem MS scans more accessible to low-abundant species to further enhance proteome coverage with limited sample input. These advantageous features led to the commercialization of a single-cell specialized IMS-MS instrumentation branded by Bruker as timsTOF SCP (Single Cell Proteomics) edition. Brunner *et al.* [80] described a single-cell proteomics workflow applying timsTOF SCP to identify proteome changes upon perturbations in HeLa cells treated with thymidine and nocodazole. Upon method optimization, treated HeLa cells were analyzed using the dia-PASEF approach and 2000 protein groups per single cell were quantifiable with median CV of 30% over all genes. Although the heterogeneity within each cell cycle stage most probably cannot be identified in routinely performed bulk sample analysis, using diaPASEF with the timsTOF SCP, correct identification of the cell's proliferation state was achieved. By comparing single-cell proteome and transcriptome data, authors have revealed stochastic changes in transcriptome, verifying the substantial regulation of transcription at single-cell level. With tandem-mass-tag labeling and carrier peptides channel, similar identification and quantification depth has been achieved with dda-PASEF acquisition, where single-cell proteomes from different cell lines (HEK-293T and HeLa) are unsupervised clustered, exhibiting the potential of proteomic differentiation of cell lines on single-cell level [81].

4.2. Intact protein analysis

Intact protein analysis is becoming increasingly significant for the comprehensive analysis of protein isoforms, particularly in targeting acidic and hydrophobic protein regions that are often underrepresented in bottom-up workflows [82]. Furthermore, IMS facilitates the elucidation of the structural characteristics of intact protein assemblies, subcomplexes, and subunits [23]. Karsen *et al.* reported on the development of a direct and high-throughput timsTOF analysis approach of cysteine-linked antibody-drug-conjugates (ADCs) within a 3

min time window [83]. The TIMS separation was fine-tuned by adjusting various parameters, including the Δ3 voltage (which influenced ion desolvation and declustering), Δ6 voltages (which affected ion trapping and release efficiency within the TIMS tunnel), the TIMS RF, and the TIMS cell collision energy. These parameters were systematically modified to acquire three levels of MS information: the first level (MS1) provided the charge-state distribution and drug-antibody ratio, the second level (MS2) offered intact mass analysis of subunits through low energy collision-induced dissociation, and the third level (MS3) enabled the determination of primary subunit sequences using high energy collision-induced dissociation.

In contrast to *N*-glycans, which exhibit structured assemblies, *O*-glycans are characterized by high heterogeneity, posing a significant analytical challenge. Roberts *et al.* successfully addressed this challenge by employing native timsTOF to elucidate the structural diversity of intact *O*-glycan proteoforms [84]. Their approach involved separating the structural heterogeneity of protein conformers within the S protein regional-binding domain. To elucidate the *O*-glycans, native PNGase F treatment was pursued allowing to remove *N*-glycans. MS1 analysis revealed the presence of two conformers (the monomer and dimer). Each conformer was fragmented using collision-activated dissociation allowing to assess the glycan structures, their localization, as well as its microheterogeneity. In combination with top-down FTICR-MS/MS, comprehensive identification of specific glycan structures and their corresponding glycosites was achieved. In a follow-up study, a novel *O*-glycosite (Thr376) unique to the SARS-CoV-2 Omicron variant was identified [85].

The analysis of high molecular weight analytes poses a significant challenge for the TIMS analyzer. This is because the TIMS mobility separation relies on immobilizing ions using an axial electrical field against the buffer gas, while a radial electrical field is simultaneously applied to prevent collisions with the electrodes. This limits the application range to approximately 150 kDa analytes. Fernandez-Lima and colleagues extended the mobility range

of TIMS analyzer for high-molecular weight species under native state by developing and implementing a convex quadrupolar TIMS in a custom-built timsTOF instrument [86]. The preservation of nativelike protein conformation was demonstrated for ubiquitin. Moreover, applicability was demonstrated for the native analysis for macromolecular assemblies with molecular weights ranging between 103 kD (concanavalin A) and 801 kDa (bacterial chaperonin GroEL), see Fig. 5 for the corresponding MS and TIMS profile. Single narrow IMS bands were observed, with an apparent mobility resolution $R \sim 80$, that indicate a high degree of structural heterogeneity of the assembly.

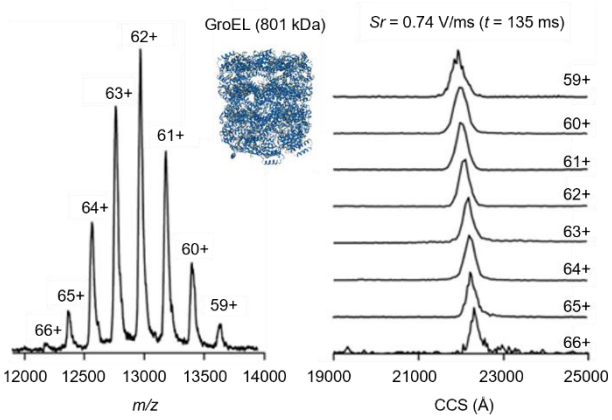

Figure 5. Native analysis the he bacterial chaperonin GroEL, which is a homo-oligomeric complex of 801 kDa composed of 14 identical subunits of 57.2 kDa appling a convex TIMS geometry coupled to TOF MS. (*Left panel*) MS1 profile of intact GroEL protein showing (*Right panel*) Correspoding TIMS collision cross-section distribution each *m/z* from 59+ to 66+. Adapted with permission from [79]. Copyright 2021. American Chemical Society.

Another ability of IM instruments is that collision induced unfolding can be performed to measure ion stabilities and to provide information on the 3D conformation, domain structure, and ligand binding [87]. By increasing the collision voltage, a protein or protein complex will trigger the unfolding (rather than dissociating bonds) resulting in a different CCS and thus a

different drift time [88]. Results obtained from these experiments are often represented in a 3D plot such as *x*-axis corresponds to the collision energy, *y*-axis to the drift time, and *z*-axis the signal intensity. Liu *et al.* reported on the development of a tandem trapped IMS analyzer (TIMS-TIMS) connected via an interface comprising two aperture plates and investigated its potential as a tool for the field of structural biology using bradykinin and ubiquitin as case studies [89]. They demonstrated the ability to collisionally-activate as well as to trap mobility selected ions, followed by subsequent mobility-analysis. Borotto *et al.* described the use of a commercial timsTOF instrument to study unfolding of native-like ions of ubiquitin, cytochrome C, β-lactoglobulin, and carbonic anhydrase, upon collisional activation [87]. Gradual increments in TIMS DC voltages led to a gradual unfolding of proteins. Although the limited transfer efficiencies restrict the analysis of proteins with native charge states exceeding 3000 Th, the resolution provided by TIMS-based mobility separations has the potential to detect previously unresolvable near-isochoric species. Fouque *et al.* explored the conformational and binding dynamics of an intrinsically disordered DNA-binding protein expressed during embryogenesis [90]. Upon DNA binding, a reduction of the conformational space and charge-state distribution was observed.

5. Concluding remarks

Over the years, ion mobility (IM) has evolved from being an independent analytical technique to being hyphenated with mass spectrometry, showing great promise for the detection and characterization of gas phase analytes in complex biological samples. As a result, it has gradually become integrated into proteomics workflows. This review aims to provide an introduction to the fundamentals of IM and discuss the pros and cons of the different modes. It also discusses key parameters such as drift time, ion mobility, collisional cross-section, and their interrelationships.

The rapid development of IM in conjunction with mass spectrometry has led to the commercialization of several IM instruments based on different modes of operation. Four notable designs, namely drift tube ion mobility spectrometry (DTIMS), high-field asymmetric-waveform ion mobility spectrometry (FAIMS), traveling-wave ion mobility spectrometry (TWIMS), and the recently emerging trapped ion mobility spectrometry (TIMS), have successfully integrated with high-resolution mass spectrometers. With its inherent operational principle, the timsTOF can be seamlessly integrated into traditional LC-MS approaches. The addition of the PASEF mode provides the ability to perform high-resolution analyses by increasing the scan ramp or to achieve high-throughput analyses by decreasing the scan ramp. Moreover, the timsTOF's capability to analyze a wide range of ion mobilities has been applied to the separation of peptides up to macro-molecular assemblies. The majority, if not all applications targeting intact protein analysis have been performed through direct injection. The incorporation of (native) LC upstream to enhance the resolving power of the analytical method is of interest. Additionally, coupling with high-resolution mass spectrometers such as the FTICR as already envisaged by Fernandez-Lima and coworkers [91], will enable the characterization of minor protein variants by further increasing the mass resolution.

6. Acknowledgements

Support of this work by a grant from the Research Foundation Flanders – FWO (grant number: G033018N) is gratefully acknowledged. SE acknowledges an Excellence of Science grant (30897864) of the Research Foundation Flanders and the Fonds de la Recherche Scientifique (FWO-FRNS).

7. Conflict of interest statement

The authors declare that they have no conflict in interest. GM is an employee at Bruker.

8. References

[1] Wrigley CW, Protein mapping by combined gel electro-focusing and electrophoresis: application to the study of genotypic variations in wheat gliadins. Biochem Genet. 1970;4:509–16.

[2] Wilkins MR, Pasquali C, Appel RD, Ou K, Golaz O, Sanchez J-C, Yan JX, Gooley AA, Hughes G, Humphery-Smith I, Williams KL, Hochstrasser DF, From proteins to proteomes: large scale protein identification by two-dimensional electrophoresis and amino acid analysis. Nat Biotechnol. 1996;14:61–5.

[3] International Human Genome Sequencing Consortium, Finishing the euchromatic sequence of the human genome. Nature. 2004;431:931–45.

[4] Omenn GS, Lane L, Overall CM, Cristea IM, Corrales FJ, Lindskog CC, Paik Y-K, Van Eyk JE, Liu S, Pennington SR, Snyder MP, Baker MS, Bandeira N, Aebersold R, Moritz RL, Deutsch EW, Research on the human proteome reaches a major milestone: > 90% of predicted human proteins now credibly detected, according to the HUPO human proteome project. J Proteome Res. 2020;19:4735–46.

[5] Omenn GS, Lane L, Overall CM, Pineau C, Packer NH, Cristea IM, Lindskog C, Weintraub ST, Orchard S, Roehrl MHA, Nice E, Liu S, Bandeira N, Chen Y-J, Guo T, Aebersold R, Moritz RL, Deutsch EW, The 2022 report on the human proteome from the HUPO human proteome project. J Proteome Res. 2023;22:1024–42.

[6] Brown KA, Melby JA, Roberts, DS, Ge Y, Top-down proteomics: challenges, innovations, and applications in basic and clinical research. Expert Rev Proteomics. 2020;17:719–33.

[7] Zhang Y, Fonslow BR, Shan B, Baek M-C, Yates JR, Protein analysis by shotgun/bottom-up proteomics. Chem Rev. 2013;113:2343–2394.

[8] Pandeswari PB, Sabareesh V, Middle-down approach: a choice to sequence and characterize proteins/proteomes by mass spectrometry. RSC Adv. 2019;9:313–44.

[9] Thomson JJ, Rutherford E, XL. On the passage of electricity through gases exposed to Röntgen rays. The London, Edinburgh, and Dublin Philosophical Magazine and Journal of Science. 1896;42:392–407.

[10] Barnes WS, Martin DW, McDaniel EW, Mass spectrographic identification of the ion observed in hydrogen mobility experiments. Phys Rev Lett. 1961;6:110–11.

[11] McAfee KB, Edelson D, Identification and mobility of ions in a townsend discharge by time-resolved mass spectrometry. Proc Phys Soc. 1963;81:382–84.

[12] Karasek FW, Cohen MJ, Carroll DI, Trace studies of alcohols in the plasma chromatograph-mass spectrometer. J Chromatogr Sci. 1971; 9:390–92.

[13] Delafield DG, Lu, G, Kaminsky CJ, Li L, High-end ion mobility mass spectrometry: A current review of analytical capacity in omics applications and structural investigations. TrAC - Trends Anal Chem. 2022;157:116761.

[14] Gabelica V, Shvartsburg AA, Afonso C, Barran P, Benesch JLP., Bleiholder C, Bowers MT, Bilbao A, Bush MF, Campbell JL, Campuzano IDG, Causon T, Clowers BH, Creaser CS, De Pauw E, Far J, Fernandez-Lima F, Fjeldsted JC, Giles K, Groessl M, Hogan CJ, Hann S, Kim HI, Kurulugama RT, May JC, McLean JA, Pagel K, Richardson K, Ridgeway ME, Rosu

F, Sobott F, Thalassinos K, Valentine SJ, Wyttenbach T, Recommendations for reporting ion mobility mass spectrometry measurements. Mass Spectrom. Rev. 2019;38:291–320.

[15] Langevin P., Une formule fondamentale de theorie cinetique. Annales de Chimie et de Physique, series. 1905;5:245–88.

[16] Mason, EA, Schamp HW, Mobility of gaseous ions in weak electric fields. Ann Phys. 1958;4:233–70.

[17] Eiceman, GA, Karpas Z, Hill HH, Ion Mobility Spectrometry. CRC Press, Boca Raton 2014.

[18] Dodds JN, Baker ES, Ion mobility spectrometry: fundamental concepts, instrumentation, applications, and the road ahead. J Am Soc Mass Spectrom. 2019;30:2185–95.

[19] Shvartsburg AA, Differential Ion Mobility Spectrometry. CRC Press 2008.

[20] Cumeras R, Figueras E, Davis CE, Baumbach JI, Gràcia I, Review on ion mobility spectrometry. Part 1: current instrumentation. Analyst. 2015;140:1376–90.

[21] D'Atri V, Causon T, Hernandez-Alba O, Mutabazi A, Veuthey J-L, Cianferani S, Guillarme D, Adding a new separation dimension to MS and LC-MS: What is the utility of ion mobility spectrometry? *J* Sep Sci. 2018;41:20–67.

[22] Lanucara F, Holman SW, Gray CJ, Eyers CE, The power of ion mobility-mass spectrometry for structural characterization and the study of conformational dynamics. Nat Chem. 2014;6:281–94.

[23] Christofi E, Barran P, Ion mobility mass spectrometry (IM-MS) for structural biology: insights gained by measuring mass, charge, and collision cross section. Chem Rev. 2023;123:2902–49.

[24] Baker ES, Clowers BH, Li F, Tang K, Tolmachev AV, Prior DC, Belov ME, Smith RD, Ion mobility spectrometry-mass spectrometry performance using electrodynamic ion funnels and elevated drift gas pressures. J Am Soc Mass Spectrom. 2007;18:1176–87.

[25] Morrison KA, Siems WF, Clowers BH, Augmenting ion trap mass spectrometers using a frequency modulated drift tube ion mobility spectrometer. Anal Chem. 2016;88:3121–29.

[26] Smith DP, Knapman TW, Campuzano I, Malham RW, Berryman JT, Radford SE, Ashcroft AE Deciphering drift time measurements from travelling wave ion mobility spectrometry-mass spectrometry studies. Eur J Mass Spectrom. 2009;15:113–30.

[27] Gabelica V, in: Ashcroft, A. E., Sobott, F. (Eds.). Royal Society of Chemistry, Cambridge 2021, pp. 1–25.rid

[28] Giles K, Ujma J, Wildgoose J, Pringle S, Richardson K, Langridge D, Green M, A cyclic ion mobility-mass spectrometry system. Anal Chem. 2019;91:8564–73.

[29] Hamid AM, Ibrahim YM, Garimella SVB, Webb IK, Deng L, Chen T-C, Anderson GA, Prost SA, Norheim RV, Tolmachev AV, Smith RD, Characterization of traveling wave ion mobility separations in structures for lossless ion manipulations. Anal Chem 2015;87:11301–08.

[30] Shvartsburg AA, Encyclopedia of Spectroscopy and Spectrometry. Elsevier 2010, pp. 1140–1148.

[31] Winter DL, Wilkins MR, Donald WA, Differential ion mobility–mass spectrometry for detailed analysis of the proteome. Trends Biotechnol. 2019;37:198–213.

[32] Fernandez-Lima FA, Kaplan DA, Park MA, Note: Integration of trapped ion mobility spectrometry with mass spectrometry. Rev Sci Instrum. 2011;82:126106.

[33] Silveira JA, Ridgeway ME, Laukien FH, Mann M, Park MA, Parallel accumulation for 100% duty cycle trapped ion mobility-mass spectrometry. Int J Mass Spectrom. 2017;413:168–75.

[34] Meier F, Beck S, Grassl N, Lubeck M, Park MA, Raether O, Mann M, Parallel accumulation–serial fragmentation (PASEF): multiplying sequencing speed and sensitivity by synchronized scans in a trapped ion mobility device. J Proteome Res. 2015;14:5378–87.

[35] Shvartsburg AA, Smith RD, Fundamentals of traveling wave ion mobility spectrometry. Anal Chem. 2008;80:9689–99.

[36] Michelmann K, Silveira JA, Ridgeway ME, Park MA, Fundamentals of trapped ion mobility spectrometry. J Am Soc Mass Spectrom. 2015;26:14–24.

[37] Gabelica V, Marklund E, Fundamentals of ion mobility spectrometry. Curr Opin Chem Biol. 2018;42:51–59.

[38] Guevremont R, High-field asymmetric waveform ion mobility spectrometry: A new tool for mass spectrometry. J Chromatogr A. 2004;1058:3–19.

[39] Dodds JN, May JC, McLean, JA, Correlating resolving power, resolution, and collision cross section: unifying cross-platform assessment of separation efficiency in ion mobility spectrometry. Anal Chem. 2017;89:12176–84.

[40] Saba J, Bonneil E, Pomiès C, Eng K, Thibault P, Enhanced sensitivity in proteomics experiments using FAIMS coupled with a hybrid linear ion trap/Orbitrap mass spectrometer. J Proteome Res. 2009;8:3355–66.

[41] Swearingen KE, Moritz RL, High-field asymmetric waveform ion mobility spectrometry for mass spectrometry-based proteomics. Expert Rev Proteomics. 2012;9:505–17.

[42] Meier F, Brunner AD, Koch S, Koch H, Lubeck M, Krause M, Goedecke N, Decker J, Kosinski T, Park MA, Bache N, Hoerning O, Cox J, Räther O, Mann M, Online parallel accumulation–serial fragmentation (PASEF) with a novel trapped ion mobility mass spectrometer. Molecular & Cellular Proteomics. 2018;17:2534–45.

[43] Meier F, Brunner A-D, Frank M, Ha A, Bludau I, Voytik E, Kaspar-Schoenefeld S, Lubeck M, Raether O, Bache N, Aebersold R, Collins BC, Röst HL, Mann M, diaPASEF: parallel accumulation–serial fragmentation combined with data-independent acquisition. Nat Methods. 2020;17:1229–36.

[44] Oliinyk D, Meier F, Ion mobility-resolved phosphoproteomics with dia-PASEF and short gradients. Proteomics. 2023;23:2200032

[45] Charkow J, Röst HL, Trapped ion mobility spectrometry reduces spectral complexity in mass spectrometry-based proteomics. Anal Chem. 2021;93:16751–58.

[46] Abramsson ML, Sahin C, Hopper JTS, Branca RMM, Danielsson J, Xu M, Chandler SA, Österlund N, Ilag LL, Leppert A, Costeira-Paulo J, Lang L, Teilum K, Laganowsky A, Benesch JLP, Oliveberg M, Robinson CV, Marklund EG, Allison TM, Winther JR, Landreh M, Charge engineering reveals the roles of ionizable side chains in electrospray ionization mass spectrometry. JACS Au. 2021;1:2385–93.

[47] Yen H, Liko I, Gault J, Wu D, Struwe WB, Robinson CV, Correlating glycoforms of DC-SIGN with stability using a combination of enzymatic digestion and ion mobility mass spectrometry. Angew Chem. 2020;132:15690–94.

[48] Ruotolo BT, Hyung S-J, Robinson PM, Giles K, Bateman RH, Robinson CV, Ion mobility–mass spectrometry reveals long-lived, unfolded intermediates in the dissociation of protein complexes. Angew Chem Int Ed. 2007;46:8001–04.

[49] Gray CJ, Thomas B, Upton R, Migas LG, Eyers CE, Barran PE, Flitsch SL, Applications of ion mobility mass spectrometry for high throughput, high resolution glycan analysis. Biochim Biophys Acta. 2016;1860:1688–1709.

[50] Szymańska E, Davies AN, Buydens LMC, Chemometrics for ion mobility spectrometry data: recent advances and future prospects. Analyst. 2016;141 5689–708.

[51] Freeke J, Bush MF, Robinson CV, Ruotolo BT, Gas-phase protein assemblies: unfolding landscapes and preserving native-like structures using noncovalent adducts. Chem Phys Lett. 2012;524:1–9.

[52] Garabedian A, Butcher D, Lippens JL, Miksovska J, Chapagain PP, Fabris D, Ridgeway ME, Park MA, Fernandez-Lima F, Structures of the kinetically trapped i-motif DNA intermediates. Phys Chem Chem Phys. 2016;18:26691–702.

[53] Valentine SJ, Ewing MA, Dilger JM, Glover MS, Geromanos S, Hughes C, Using ion mobility data to improve peptide identification: intrinsic amino acid size parameters. J Proteome Res. 2011;10:2318–29.

[54] Fernandez-Lima F, Kaplan DA, Suetering J, Park MA, Gas-phase separation using a trapped ion mobility spectrometer. Int J Ion Mobil Spectrom. 2011;14:93–98.

[55] Fernandez-Lima FA, Kaplan DA, Park MA, Note: Integration of trapped ion mobility spectrometry with mass spectrometry. Rev Sci Instrum. 2011;82:126106.

[56] Ridgeway ME, Bleiholder C, Mann M, Park MA, Trends in trapped ion mobility-mass spectrometry instrumentation. TrAC - Trends Anal Chem. 2019;116:324–31.

[57] Jeanne Dit Fouque K, Fernandez-Lima F, Recent advances in biological separations using trapped ion mobility spectrometry-mass spectrometry. TrAC - Trends Anal Chem. 2019;116:308–15.

[58] Ridgeway ME, Lubeck M, Jordens J, Mann M, Park MA, Trapped ion mobility spectrometry: a short review. Int J Mass Spectrom. 2018;425:22–35.

[59] Loboda A, Novel ion mobility setup combined with collision cell and time-of-flight mass spectrometer. J Am Soc Mass Spectrom. 2006;17:691–99.

[60] Bleiholder C, Towards measuring ion mobilities in non-stationary gases and non-uniform and dynamic electric fields (I). Transport equation. Int J Mass Spectrom. 2016,399–400:1–9.

[61] Benigni P, Porter J, Ridgeway Mark E, Park Melvin A, Fernandez-Lima F, Increasing analytical separation and duty cycle with nonlinear analytical mobility scan functions in TIMS-FT-ICR MS. Anal Chem. 2018;90:2446–50.

[62] Hernandez DR, DeBord JD, Ridgeway ME, Kaplan DA, Park MA, Fernandez-Lima F, Ion dynamics in a trapped ion mobility spectrometer. Analyst. 2014;139:1913–21.

[63] Silveira JA, Michelmann K, Ridgeway ME, Park MA, Fundamentals of trapped ion mobility spectrometry part II: fluid dynamics. J Am Soc Mass Spectrom. 2016;27:585–95.

[64] Silveira JA, Ridgeway ME, Laukien FH, Mann M, Park MA, Parallel accumulation for 100% duty cycle trapped ion mobility-mass spectrometry. Int J Mass Spectrom. 2017;413:168–75.

[65] Michelmann K, Silveira JA, Ridgeway ME, Park MA, Fundamentals of trapped ion mobility spectrometry. J Am Soc Mass Spectrom. 2015;26:14–24.

[66] Venable JD, Dong M-Q, Wohlschlegel J, Dillin A, Yates JR, Automated approach for quantitative analysis of complex peptide mixtures from tandem mass spectra. Nat Methods. 2004;1:39–45.

[67] Demichev V, Szyrwiel L, Yu F, Teo GC, Rosenberger G, Niewienda A, Ludwig D, Decker J, Kaspar-Schoenefeld S, Lilley KS, Mülleder M, Nesvizhskii AI, Ralser M, dia-PASEF data analysis using FragPipe and DIA-NN for deep proteomics of low sample amounts. Nat Commun. 2022;13:3944.

[68] Szyrwiel L, Sinn L, Ralser M, Demichev V, Slice-PASEF: fragmenting all ions for maximum sensitivity in proteomics. bioRxiv. 2022.

[69] Skowronek P, Krohs F, Lubeck M, Wallmann G, Itang ECM, Koval P, Wahle M, Thielert M, Meier F, Willems S, Raether O, Mann M, Synchro-PASEF allows precursor-specific fragment ion extraction and interference removal in data-independent acquisition. Mol Cell Biol. 2023;22:100489.

[70] Distler U, Krzysztof M, Startek MP, Teschner D, Brehmer S, Decker J, Schild T, Krieger J, Krohs F, Raether O, Hildebrandt A, Tenzer S, midiaPASEF maximizes information content in data-independent acquisition proteomics. BioRxiv 2023.

[71] Yates JR, Ruse CI, Nakorchevsky A, Proteomics by Mass Spectrometry: Approaches, Advances, and Applications. Annu Rev Biomed Eng. 2009;11:49–79.

[72] Meier F, Park MA, Mann M, Trapped ion mobility spectrometry and parallel accumulation–serial fragmentation in proteomics. Mol Cell Proteomics. 2021;20:100138.

[73] Link AJ, Eng J, Schieltz DM, Carmack E, Mize GJ, Morris DR, Garvik BM, Yates JR, Direct analysis of protein complexes using mass spectrometry. Nat Biotechnol. 1999;17:676–82.

[74] Scheltema RA, Hauschild J-P, Lange O, Hornburg D, Denisov E, Damoc E, Kuehn A, Makarov A, Mann M, The Q Exactive HF, a benchtop mass spectrometer with a pre-filter, high-performance quadrupole and an ultra-high-field Orbitrap analyzer. Molecular & Cellular Proteomics. 2014;13:3698–708.

[75] Sandow JJ, Infusini G, Dagley LF, Larsen R, Webb AI, Hall E, Simplified high-throughput methods for deep proteome analysis on the timsTOF Pro. *BioRxiv.* 2021.

[76] Szyrwiel L, Gille C, Mülleder M, Demichev V, Ralser M, Speedy-PASEF: analytical flow rate chromatography and trapped ion mobility for deep high-throughput proteomics. *BioRxiv*. 2023.

[77] Tomioka A, Tomioka R, Mori I, Isobe Y, Arita M, Imami K, Kanao E, Ogata K, Ishihama Y, One thousand samples per day capillary-flow LC/MS/MS for high-speed, high-sensitivity and in-depth proteomics. *BioRxiv.* 2023.

[78] Eshghi A, Xie X, Hardie D, Chen MX, Izaguirre F, Newman R, Zhu Y, Kelly RT, Goodlett DR, Sample preparation methods for targeted single-cell proteomics. J Proteome Res. 2023;22:1589–602.

[79] Røberg-Larsen H, Lundanes E, Nyman TA, Berven FS, Wilson SR, Liquid chromatography, a key tool for the advancement of single-cell omics analysis. Anal Chim Acta. 2021;1178:338551.

[80] Brunner A, Thielert M, Vasilopoulou C, Ammar C, Coscia F, Mund A, Hoerning OB, Bache N, Apalategui A, Lubeck M, Richter S, Fischer DS, Raether O, Park MA, Meier F, Theis FJ, Mann M, Ultra-high sensitivity mass spectrometry quantifies single-cell proteome changes upon perturbation. Mol Syst Biol. 2022;18:e10798.

[81] Lei Gu A, Li Z, Wang Q, Zhang H, Sun Y, Li C, Wang H, An ultra-sensitive and easy-to-use multiplexed single-cell proteomic analysis. *BioRxiv.* 2022.

[82] Dupree EJ, Jayathirtha M, Yorkey H, Mihasan M, Petre BA, Darie CC, A critical review of bottom-up proteomics: the good, the dad, and the future of this field. Proteomes. 2020;8:14.

[83] Larson EJ, Roberts DS, Melby JA, Buck KM, Zhu Y, Zhou S, Han L, Zhang Q, Ge Y, High-throughput multi-attribute analysis of antibody-drug conjugates enabled by trapped ion mobility spectrometry and top-down mass spectrometry. Anal Chem. 2021;93:10013–21.

[84] Roberts DS, Mann M, Melby JA, Larson EJ, Zhu Y, Brasier AR, Jin S, Ge Y, Structural O-glycoform heterogeneity of the SARS-CoV-2 spike protein receptor-binding domain revealed by top-down mass spectrometry. J Am Chem Soc. 2021;143:12014–24.

[85] Roberts DS, Mann M, Li BH, Kim D, Braiser AR, Jin S, Ge Y, Distinct core glycan and *O* -glycoform utilization of SARS-CoV-2 Omicron variant spike protein RBD revealed by top-down mass spectrometry. Chem Sci. 2022;13:0944–49.

[86] Jeanne Dit Fouque K, Garabedian A, Leng F, Tse-Dinh Y-C, Ridgeway ME, Park MA, Fernandez-Lima F, Trapped ion mobility spectrometry of native macromolecular assemblies. Anal Chem. 2021;93:2933–41.

[87] Borotto NB, Osho KE, Richards TK, Graham KA, Collision-induced unfolding of native-like protein ions within a trapped ion mobility spectrometry device. J Am Soc Mass Spectrom. 2022;33:83–89.

[88] Dixit SM, Polasky DA, Ruotolo BT, Collision induced unfolding of isolated proteins in the gas phase: past, present, and future. Curr Opin Chem Biol. 2018;42:93–100.

[89] Liu FC, Ridgeway ME, Park MA, Bleiholder C, Tandem trapped ion mobility spectrometry. Analyst. 2018;143 2249–58.

[90] Jeanne Dit Fouque K, Sipe SN, Garabedian A, Mejia G, Su L, Hossen ML, Chapagain PP, Leng F, Brodbelt JS, Fernandez-Lima F, Exploring the conformational and binding dynamics of HMGA2·DNA complexes using trapped ion mobility spectrometry–mass spectrometry. J Am Soc Mass Spectrom. 2022;33:1103–12.

[91] Tose LV, Benigni P, Leyva D, Sundberg A, Ramírez CE, Ridgeway ME, Park MA, Romão W, Jaffé R, Fernandez-Lima F, Coupling trapped ion mobility spectrometry to mass spectrometry: trapped ion mobility spectrometry–time-of-flight mass spectrometry versus trapped ion mobility spectrometry - Fourier transform ion cyclotron resonance mass spectrometry. Rapid Commun. Mass Spectrom. 2018;32:1287–95.

[92] Meier F, Beck S, Grassl N, Lubeck M, Park MA, Raether O, Mann M, Parallel accumulation–serial fragmentation (PASEF): multiplying sequencing speed and sensitivity by synchronized scans in a trapped ion mobility device. J Proteome Res. 2015;14:5378–87.